Improved Aerodynamic Characterization of Regular Three-Dimensional Roughness

D. R. Waigh* and R. J. Kind†
Carleton University, Ottawa, Ontario K1S 5B6, Canada

Introduction

SURFACE roughness can seriously degrade the lift-and-drag performance of airfoils, wings, and turbomachinery blading. The ability to predict its effects is therefore important, and this generally requires computation of the viscous flow over the body. The two most common approaches for the viscous computations are to use wall functions, i.e., the law of the wall with modifications to represent roughness effects, for the near-wall flow or to integrate the equations of motion from the wall using a turbulence model that includes a correlation for roughness effects. Examples of the latter are found in Ref. 1, the Wilcox[2] k-ω model, and the Zhang et al.[3] k-ε model. In both the wall-function and the turbulence-model approaches, it is necessary to characterize the actual roughness either in terms of its standard-sand height k_s or, equivalently, in terms of the shift C that it produces in the law-of-the-wall intercept. The present Note addresses this question by examining the correlation between the geometry of regular arrays of three-dimensional roughness elements and the shift C.

Theory and Analysis

The direct effects of roughness appear in the inner region of the turbulent boundary layer ($y/\delta < 0.2$) (Ref. 4). The logarithmic law of the wall describes most of the flow in this region. For surfaces that are "fully rough" in the aerodynamic sense, the logarithmic law of the wall can be expressed, using the conventional notation, as[4]

$$u/u_\tau = A \ln(y/k) + B - C \tag{1}$$

where A and B are empirical constants whose values, 1/0.41 and 5.0, respectively, have been well established from smooth-wall experiments.[5] The roughness constant C is also determined empirically but unlike A and B is dependent on geometric properties of the roughness. Establishing a value for C amounts to aerodynamic characterization of any given roughness configuration because Eq. (1) is then fully defined. The value of C for standard sand is -4.0 (Ref. 6); thus, using Eq. (1),

$$k_s/k = \exp[(C + 4)/A] \tag{2}$$

The present study tries to better relate the effects of roughness geometry to the roughness constant C. Our approach builds mainly on the work of Dvorak,[7] Simpson,[8] and Dirling.[9] A database was constructed describing the experimental results and the geometry of 64 rough surfaces previously investigated in 16 separate low-speed wind tunnel experiments; the reevaluation[10] of some of Schlichting's data was also included. The database covers a wide range of roughness element shapes (cubes, blocks, flat plates, cylinders, rods, cones, spheres, and hemispheres) and distributions in fully rough flow conditions. Details are available in Ref. 11.

Roughness geometry was characterized by describing two different aspects of it: roughness element distribution, which characterizes the interelement geometry, and roughness element shape, which characterizes the geometry of the individual elements.

Three parameters were used to describe the element distribution (see Fig. 1 for notation):

Spacing parameter $\lambda = A_S/A_F$. This is the spacing parameter proposed by Simpson[8]; it has been proven to influence the roughness constant.

Cell aspect ratio $\beta = L/M$. It was thought that closer spanwise spacing would force flow over the elements and affect drag.

Stagger parameter $\gamma = m/M$.

Three more parameters were used to nondimensionalize the geometry of individual roughness elements (see Fig. 1b for notation):

Bluntness parameter A_W/A_F. This parameter, the reciprocal of that originally proposed by Dirling,[9] measures the "bluntness" of the roughness elements; increasing A_W/A_F corresponds to more rounded elements whose drag is expected to be lower.

Spanwise aspect ratio k/b_m.

Streamwise aspect ratio k/s_m.

When the experimental data for the roughness constant C are plotted against the spacing parameter λ, there is considerable scatter; uncertainty varies from about $\pm 1\frac{1}{2}$ for $\lambda < 5$ to about ± 3 for $\lambda > 5$. Values of the coefficients of determination r^2 of best straight-line fits to the C vs λ data are 0.74 for $\lambda < 5$ and 0.71 for $\lambda > 5$. To improve upon this fit, it was proposed to plot the roughness-constant data against a multivariable effective spacing parameter that combined λ with some of the other geometric descriptors. Several effective spacing parameters were evaluated using a computerized optimization process. This required minimization of the sum of the squares of the errors between each experimentally determined value of C in the database and the value given by a correlation of the form

$$C = a \log_{10}\left(\lambda X_1^c X_2^d\right) + b \tag{3}$$

where X_1 and X_2 are geometric descriptors (like β or k/b_m) and a, b, c, and d are "constants" adjusted to minimize the sum of the squared errors. The stagger parameter γ has values of either 0 or $\frac{1}{2}$, and the zero value would have disrupted the logarithmic roughness model. The effect of stagger was therefore assessed visually by inspection of separate plots, one for $\gamma = 0$ and the other for $\gamma = \frac{1}{2}$. Two-dimensional roughness elements were excluded from the database for similar reasons: Their spanwise aspect ratio k/b_m is equal to zero, which would also have disrupted the logarithmic calculations.

Previous researchers have found that roughness falls into two different spacing regimes, referred to herein as the *dense* and *sparse regimes*, corresponding to low and high values of λ, respectively.[7,8] Experimental values of the roughness constant C are found to increase with increasing λ in the dense regime and vice versa in the sparse regime. In the dense regime, the closely spaced roughness elements do not let much flow pass between them but instead force the flow to skim over the top of the roughness array. Increasing the space between roughness elements in the dense spacing regime will decrease the shelter effect experienced by individual elements and

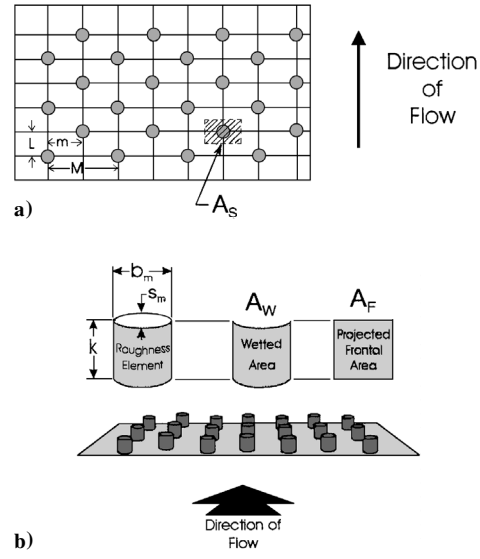

Fig. 1 Geometry of a rough wall. (Note that A_W is the upstream-facing wetted area of an element.)

Received July 20, 1997; revision received Feb. 4, 1998; accepted for publication Feb. 19, 1998.

*Graduate Student, Department of Mechanical and Aerospace Engineering.

†Professor, Department of Mechanical and Aerospace Engineering. Associate Fellow AIAA.

will thus increase drag. In the sparse regime, on the other hand, the flow passes between the roughness elements and impinges more directly on each roughness element. Drag then tends to be directly proportional to the number of roughness elements and decreases if this number is decreased, that is, if the spacing λ is increased. The data must thus be divided into two groups with separate correlation relations fitted to each group.

Unfortunately, λ does not serve as a good discriminator between the dense and sparse spacing regimes: For λ near 5 there is much scatter in the data, and some of it appears to correspond to the dense regime and some to the sparse regime. Because the spacing regime depends on the size of the intervening spaces between roughness elements, a new parameter Λ measuring these spaces was introduced:

$$\Lambda = \frac{\text{Total volume over surface (to height } k)}{\text{Effective volume of roughness elements}} = \frac{A_S k}{b_m k s_m} = \frac{A_S k}{A_F S_m} = \lambda \frac{k}{s_m} \tag{4}$$

Smaller values of Λ thus correspond to relatively less intervening space between roughness elements and vice versa.

It was found that Λ did serve as a good discriminator between spacing regimes, with $\Lambda < 6$ corresponding to the dense regime, i.e., $dC/d\Lambda$ positive, and $\Lambda > 6$ to the sparse regime, i.e., $dC/d\Lambda$ negative.[11] The significance of Λ is illustrated by the thin-rod data for which $\lambda < 3$ and $\Lambda > 50$; these data are in the sparse regime because the flow readily passes between the relatively wide spaces separating the rods.

Results

Although several different effective spacing parameters were studied, one particular roughness function gave a significant improvement in the prediction of the roughness constant C in both spacing regimes. This function used the element bluntness A_W/A_F, spanwise aspect ratio k/b_m, and relative spacing λ. In the dense spacing regime ($\Lambda < 6$), this led to the following correlation for the roughness constant:

$$C = 10.56 \log_{10} \left[\lambda (k/b_m)^{0.87} (A_W/A_F)^{0.44} \right] - 7.59 \tag{5}$$

The experimental data fit this correlation with a coefficient of determination $r^2 = 0.95$ and, with a probability of 95%, an uncertainty of about ± 1 (Fig. 2a). In the sparse regime ($\Lambda > 6$), the optimization process yielded the correlation

$$C = -5.75 \log_{10} \left[\lambda (k/b_m)^{0.55} (A_W/A_F)^{1.38} \right] + 5.78 \tag{6}$$

which fits the experimental data with a coefficient of determination of $r^2 = 0.91$ and an uncertainty of about $\pm 1\frac{1}{2}$ (Fig. 2b). All effective spacing parameters based on other combinations of geometric parameters produced considerably poorer correlations.[11] Note from Fig. 2 that, when λ_{eff} is between about 2 and 10, the dense and sparse regimes overlap; that is, the roughness can be either dense or sparse, depending on its value of Λ.

Most of the roughness elements studied had equal spanwise and streamwise aspect ratios, k/b_m and k/s_m, respectively; only 11 of the 64 data points did not. An effective spacing parameter that used k/s_m instead of k/b_m was not as successful in reducing scatter as were Eqs. (5) and (6). More data for roughness with $k/s_m \not\approx k/b_m$ would be required to investigate the effects, if any, of streamwise aspect ratio k/s_m.

Surprisingly, neither cell aspect ratio nor stagger was found to affect the roughness constant significantly,[11] indicating that the roughness constant is insensitive to the pattern of the roughness array.

The present work was confined to experiments with simple roughness element shapes arranged in regular patterns. It would be necessary to find ways to parameterize the geometry of natural roughness effectively to apply the present results to it. Kind and Lawrysyn[12] and Kind et al.[13] had some success in this regard using appropriately defined mean values of k and λ in an earlier correlation for C. It should also be possible to define suitable mean values of b_m and A_W for natural roughness of various types, thus allowing the improved correlations, Eq. (5) or (6), to be used. The prospects for success are enhanced by the finding that neither cell aspect ratio nor stagger is important.

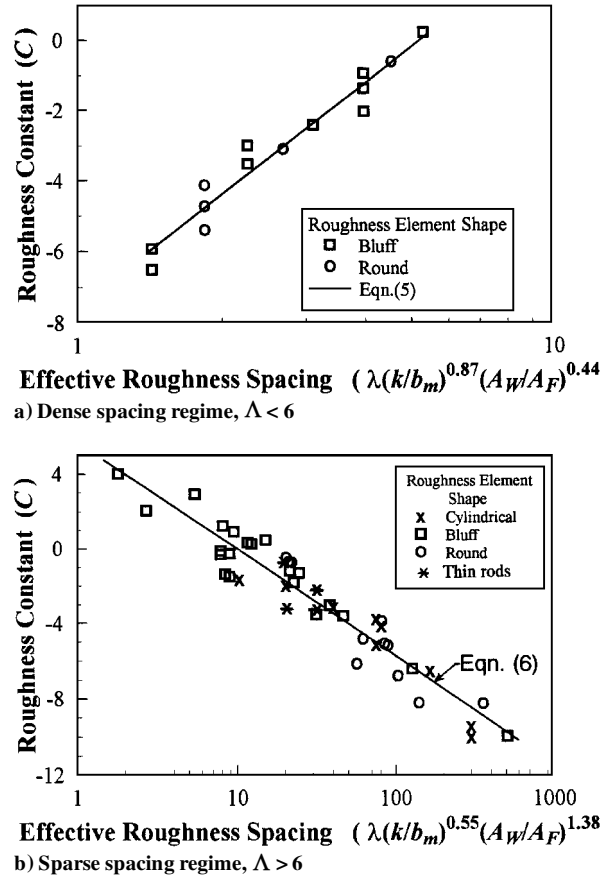

Fig. 2 Experimental values of the roughness constant vs effective spacing parameter: Bluff = flat plates and blocks; Round = spheres, hemispheres, spherical segments, and cones.

Conclusions

Improvements in characterizing regular roughness can be made by accounting for the shape of the roughness elements. A measure of element bluntness and the spanwise aspect ratio are used. New correlations that reduce uncertainty by a factor of about 2 have been presented. The pattern in which roughness elements are arranged does not appear to affect the roughness constant significantly. A criterion for distinguishing between the dense and sparse spacing regimes has been presented.

Acknowledgment

This work was supported by the Natural Sciences and Engineering Research Council of Canada through a research grant.

References

[1] Cebeci, T., and Chang, K. C., "Calculation of Incompressible Rough-Wall Boundary-Layer Flows," *AIAA Journal*, Vol. 16, No. 7, 1978, pp. 730–735.

[2] Wilcox, D. C., "Reassessment of the Scale-Determining Equation for Advanced Turbulence Models," *AIAA Journal*, Vol. 26, No. 11, 1988, pp. 1299–1310.

[3] Zhang, H., Faghri, M., and White, F. M., "A New Low-Reynolds-Number k-ε Model for Turbulent Flow Over Smooth and Rough Surfaces," *Journal of Fluids Engineering*, Vol. 118, June 1996, pp. 255–259.

[4] White, F. M., *Viscous Fluid Flow*, 2nd ed., McGraw–Hill, New York, 1991, Chap. 6.

[5] Coles, D., *The Young Person's Guide to the Data*, Vol. 2, AFOSR–IFP Stanford Conf. on the Calculation of Turbulent Boundary Layers, Thermosciences Div., Dept. of Mechanical Engineering, Stanford Univ., Stanford, CA, 1968, pp. 1–45.

[6] Grigson, G. W. B., "Nikuradse's Experiment," *AIAA Journal*, Vol. 22, No. 7, 1984, pp. 1000, 1001.

[7]Dvorak, F. A., "Calculation of Turbulent Boundary Layers on Rough Surfaces in Pressure Gradient," *AIAA Journal*, Vol. 7, No. 9, 1969, pp. 1752–1759.

[8]Simpson, R. L., "A Generalized Correlation of Roughness Density Effects on the Turbulent Boundary Layer," *AIAA Journal*, Vol. 11, No. 2, 1973, pp. 242–244.

[9]Dirling, R. B., "A Method for Computing Roughwall Heat Transfer Rates on Re-Entry Nosetips," AIAA Paper 73-763, July 1973.

[10]Coleman, H. W., Hodge, B. K., and Taylor, R. P., "A Re-Evaluation of Schlichting's Surface Roughness Experiment," *Journal of Fluids Engineering*, Vol. 106, March 1984, pp. 60–65.

[11]Waigh, D. R., "An Improved Correlation for Representing Surface Roughness Effects on the Law of the Wall in Fully Rough Conditions," M.Eng. Thesis, Dept. of Mechanical and Aerospace Engineering, Carleton Univ., Ottawa, ON, Canada, Sept. 1996.

[12]Kind, R. J., and Lawrysyn, M. A., "Aerodynamic Characteristics of Hoar-Frost Roughness," *AIAA Journal*, Vol. 30, No. 7, 1992, pp. 1703–1707.

[13]Kind, R. J., Serjak, P. J., and Abbott, M. W. P., "Measurements and Prediction of the Effects of Surface Roughness on Profile Losses and Deviation in Turbine Cascades," *Journal of Turbomachinery*, Vol. 120, Jan. 1998, pp. 20–27.

C. G. Speziale
Associate Editor